The pathway to drive decompression microbubbles from the tissues to the blood and the lymphatic system as a part of this transfer

J. HUGON[1], L. BARTHELEMY[3], J.C. ROSTAIN[1], B. GARDETTE[2]

[1]Université de la Méditerranée, UMR - MD2, P2COE, Institut de Neuroscience J. Roche, Faculté de Médecine Nord, 13916 Marseille Cedex 20 France; [2]COMEX SA 36 bd des Océans 13275 Marseille Cedex 9 France; [3]171, Rue Revel, 83000 Toulon France

Abstract

The formation sites of the microbubbles that are routinely detected in the bloodstream at precordial level by Doppler after a decompression are reviewed and discussed here. First, microbubbles could form on the endothelium lumen wall of the capillaries, at specific nanometric sites, but the release mechanism of such small emerging entities remains puzzling. They could be also formed from pre-existing gas nuclei present in the blood when favorable local hydrodynamic/supersaturation conditions generate micro-cavitation and tribonucleation phenomena. Finally, tissues could represent large pools for microbubble formation and amplification. Nevertheless, it remains to explain what the potential pathways are to drive them to the blood.

Knowing that the permeability of most of the blood capillary network is quite low, an alternative is proposed for such transport. The lymphatic system, which drains the interstitial fluid to guarantee the fluid balance of tissues, could allow the transfer of micrometric elements like stabilized microbubbles formed in tissues on long distances. A final rejection in the bloodstream at the termination of both right lymphatic and thoracic ducts can be expected. The characteristics of this slow transport, activated by the muscular pump, could explain the detection on long periods of massive venous gas emboli.

INTRODUCTION

Decompression sickness is characterized by a wide variety of symptoms. The associated injury can be reversible and mild but also severe and definite. In spite of more than a century of investigations, the mechanisms underlying and leading to the different forms of decompression sickness are far from being clear. The only element on which there is an agreement among the scientific community is the fact that microbubble formation during decompression is the primary event.

Accordingly, the decompression procedures used by scuba divers are the only efficient way currently known to limit the production and growth of microbubbles during and after the ascent. In this context, one of the only means that we currently have to determine the severity of a procedure on a given subject consists in the detection of the bubbles circulating in the bloodstream by using a pulsating or continuous Doppler. This latter method of investigation is widely used. Several studies have shown (1,2,3,4,5,6) that the probability of developing symptoms is linked to the quantity of moving bubbles that we can hear at the heart level.

Several theories could support this correlation. For instance, it has been proposed that the circulating microbubbles are filtered by the lung as long as their total flow rate does not exceed a given threshold above which they can cross this barrier, reach the arterial side and potentially create an embolus in a critical tissue (7,8). Secondly, the biochemical events consecutive to blood/bubbles and endothelium/bubbles interactions are sufficient to expect that avoiding large amounts of bubbles in the bloodstream will prevent, to some extent, serious symptoms of decompression sickness (9).

It has been proved by Doppler that the circulating bubbles are mainly present in the venous side of the blood circulation. While the local supersaturation circumstances under which the gas nuclei dispersed

in the body can be recruited to grow in microbubbles remain of primary interest, the mechanisms to describe how and when they can be transferred in this side of the bloodstream are also particularly interesting. Indeed, all attempts to model the mechanisms of decompression for prevention purposes need to choose the right hypothesis and criteria and be physically and physiologically consistent. In several dynamic modeling approaches, microbubbles are assumed to be located in tissues (10,11,12), but their opportunity to be rejected in the bloodstream and their further evolution are barely considered (13,14). That is why it makes sense to understand not only the gas exchange kinetics in the tissues but also the gas exchanges between the microbubbles and the blood coupled with their transport kinetics. An investigation of the dynamic characteristic of the Doppler microbubble detection signals after decompression (first appearance, peak, signal progressive drop) shall be, in that sense, instructive.

This paper reviews and discusses the different possibilities proposed in the literature for what happens at the sites of microbubble formation, with their potential release in the venous bloodstream. It presents an original hypothesis that seems compatible with different experimental facts: It is proposed that the microbubbles are mainly formed in the tissues and are transported to the blood by the lymphatic vessels.

REVIEW OF THE POTENTIAL PRIMARY SITES FOR MICROBUBBLE FORMATION

From a physical and biochemical point of view, explaining where and in which conditions microbubbles can form in the different biological media is far from evident. Homogeneous and heterogeneous nucleation hypotheses have been investigated – both theoretically and experimentally – and widely used by several authors to explain and model the bubble formation during decompression (15,16,17,18).

Even if the surface physics (surface tension and surfactant skin) and the local supersaturation states are known to be of primary importance to explain the presence and the growth capacity of pre-existing micronuclei, no one has really described with certainty where the bubbles detected by Doppler in the right side of the heart are primarily formed.

The capillaries' endothelium as a potential site

Microbubbles could form on the lumen wall of the capillaries (19,20) even if it is known that the endothelium surface facing the blood is mainly hydrophilic (16,19). The associated hydrophobic crevice model has been studied by several authors (16,17,14). The geometrical and biochemical factors required to allow such bubble release have been pointed out.

This hypothesis is nevertheless questionable if one considers the nanometric dimensions of the structures that would be involved – i.e., caveolae (21) of 50 to 100 nm in diameter. Indeed, the small gas pockets, which grow during a decompression due to the ambient pressure decrease but also because of inert gas diffusion from the neighboring supersaturated tissues, finally have to face the strong surface tension effect once their curvature reverses. The Laplace law should drastically limit the opportunity to release such small bubbles in the bloodstream.

This limitation is well known in the evaporation field: The superheating required to promote boiling of a liquid in contact with a heated wall is all the more important that the dimensions of the nucleation sites are small. Moreover, Ligier-Belair (22) has recently presented the conditions allowing massive microbubble formation from cellulose fibers immersed in carbonated beverages: Both the ambient pressure and the micrometric fibers' lumen dimension are critical parameters regulating the bubbling frequency.

To illustrate this fact, we could mention once more the recent work by Chappell and Payne concerning the modeling of endothelial bubbles formation (14): In their approach, they are forced to choose very low surface tensions to model the bubble release from nanometric sites. This hypothesis remains questionable.

Favorable hydrodynamic conditions and the cardiac valves hypothesis

Another possibility could be bubble formation directly in the circulating blood when a characteristic hydrodynamic/blood gas content conformation occurs locally: a non-negligible local pressure drop combined to a high supersaturation state of the blood. The tribonucleation phenomena (23,24,25) occurring during the opening and closing mechanisms of capillaries is, for instance, an interesting hypothesis, while poorly investigated.

A stronger hydrodynamic possibility has been described by Hennessy in 1987 (8), who proposed the cardiac valves as potential formation sites for microbubbles. He considered that gaseous cavitation could occur during the valves' closure, mainly because of vibrations at the valve tip levels. During the first minutes of a decompression, the high supersaturation state of the mixed venous blood could indeed allow the feeding of the small gas seeds so produced with inert gas, leading to microbubbles growth with a prolonged lifetime in the pulmonary artery.

This hypothesis should concern mainly tricuspid and pulmonary valves because, with the exception of abnormal lung shunt levels (2% in normal subjects), the blood leaving the lungs is not supersaturated to a great extent (with perhaps the exception of high-pressure saturation dives). This original idea could find interesting supporting proofs in the mechanical heart valves (MHV) field. Indeed, mitral and aortic mechanical valves are known to generate bubbles that can lead to various disorders for patients. The squeeze flow generated during the valves' closure at their tips and the associated vaporous cavitation phenomenon have been largely explained and investigated by numerous authors, in vivo and in vitro, for several types of valves (26,27,28,29,30,31,32). Nevertheless, the natural and healthy cardiac valves located in the right heart do not seem to fulfill in their normal function the fluid dynamic preconditions for cavitation (the closing dynamics of the natural valves are far from being as extreme as those seen for mechanical heart valves where cavitation has been demonstrated).

Moreover, it is well known that the cavitation phenomena arise only if gas seeds are already present in the circulating fluid (33). So, microcavitation at cardiac valves, if it exists, probably doesn't create micronuclei but instead amplifies pre-existing gas nuclei naturally present in the blood. How they are formed and stabilized remain questions. It would be interesting to know if studies on human blood, which contains several kind of nano to micro components (red cells, white cells, platelets, proteins), have led to the conclusion that gas nuclei are always present in such an organic fluid.

According to Harvey (15), who decompressed blood samples of cats below the blood vapor pressure at 38°C without creating bubbles, it seems to be far from sure that blood is a gas nuclei reservoir. It is interesting to notice here the conclusion of this author:

"These experiments indicate that all the formed elements of the blood (red and white corpuscles, platelets, fat globules or blood dust) play no part in bubble formation, that air masses do not normally pass from alveoli to lung capillaries (although they may when the alveolar air pressure is raised above that in the capillaries) and that movement of the blood with turbulence and vortex formation around the valves of the heart does not normally start bubble formation."

Besides, if the pre-existing stabilized gas nuclei (sub-micrometric dimensions) investigated by Yount during his experiments on decompressed gelatin samples (34,35,36,37) were present in the blood, it would be also very interesting to know what the interaction of these nuclei would be with proteins, platelets and macrophages. At any rate, cavitation at the level of the cardiac valve is probably not at the origin of the supposed nuclei present in the blood (a realistic prerequisite since mechanical heart valves can cavitate) but only a kind of amplifier that could produce gas microbubbles.

If we assume that the microbubbles are generated in the blood at the cardiac valves' level, it should have a great impact in limiting the mixed venous blood supersaturation level, while at the same time keeping the ambient pressure rather high in order to limit their production and growth. Indeed, the smaller the dimensions of the nuclei primarily recruited, the higher the level of blood supersaturation required to face the surface tension effects. And it is probable fact that the smaller the nuclei recruited, the larger the nuclei population involved and the final bubble volume.

Moreover, their subsequent growth rate is all the more important because:

1) this supersaturation level is high; and
2) the ambient pressure is low.

Because the contribution of the fast tissues (brain, liver, kidneys, heart) to the mixed venous inert gas content is probably important, the involvement of these tissues during the first minutes of a decompression should be crucial if we follow Hennessy's reasoning. This phase, including the ascent, should indeed be critical, and deep stages should be recommended to avoid high mixed venous blood su-

persaturation states and to limit microbubble growth. Theoretical elements can be found in the Annex to justify this deduction.

This last consequence, i.e., the deep stages requirement, is in phase with Hills' and Yount's (38,39) theoretical recommendations, introducing with others the modern bubbles models and the deep stages concept. Deep stages are nevertheless a current subject of controversy (40).

Microbubbles formation sites inside the tissues and the transport issue

Microbubbles could finally form *in situ*, in the tissues (more or less fat), and, among several hypotheses:

1) directly inside the cells, where the gas diffusion properties could be very low (38);
2) in the interstitial fluid, at the level of cell contact (41);
3) directly in the bulk of the interstitial media if we assume that gas nuclei always exist at this level, stabilized by surface-active skins (42).

In the case of micronuclei formed at the level of cell contact, the tribonucleation phenomenon – that we could suspect in muscles and joint mainly – and the heterogeneous nucleation could compete. But whatever the mechanisms involved in their formation, it remains yet to explain how the microbubbles are transported from the tissues to the bloodstream.

The direct transport of microbubbles across the endothelial wall is unlikely in most parts of the body because the capillary network is of a continuous type. Present in the skin, in all types of muscles, in mesenteries, in the central nervous system and the lung, such capillaries are characterized by a continuous endothelial lining with tight intercellular junctions. A passive transport of gas nuclei through these small gaps or a potential transcytosis mechanism (43, 44) would only release nanometric elements in the bloodstream, which introduces once more the crushing surface tension issue discussed just above for caveolae.

It is well known that capillary permeability, all transcapillary exchange routes for macromolecules being considered (interendothelial clefts, vesicular transport, channel formed by plasmalemmal vesicles), remains quite low (45). Large elements like leukocytes can pass through the endothelium of the continuous capillary network, but very specialized biochemical mechanisms are involved (46).

This specific transport path seems nevertheless excluded for foreign microbubbles. Finally, effraction of the capillary endothelium is a non-realistic hypothesis, because serious clinical signs would be expected if one considers the great flow rate of bubbles detected in the venous blood by Doppler during several hours following a decompression, often without any symptoms detected.

Two other types of capillaries exist: the fenestrated and the sinusoidal. They may offer a greater permeability level because larger clefts for the transport can be found at the level of the endothelium. The fenestrated capillaries offer gaps having dimensions up to 100 nm and are found in endocrine and exocrine glands, gastric and intestinal mucosae, choroid plexuses of the brain, renal tubules and glomureli and in the ciliary body of the eyes (47).

The sinusoidal capillaries, characterized by an incomplete basal lamina, allow the passage of micrometric elements like blood cells into the liver and in the spleen. The fact that all the tissues concerned by such permeable capillaries are fast tissues is not incompatible with the fact that slow tissues are involved in decompression sickness: Gas nuclei could be generated at this level, could pass into the blood during the first minutes of a decompression, then amplified in the supersaturated mixed venous blood up to the pulmonary filter.

But these well-vascularized tissues desaturate quickly. As a consequence, it can be expected that if they are microbubbls providers, it is only on a short period of time. A slow ascent should drastically decrease the microbubbles production in theses fast tissues (T1/2≈1min) and limit their subsequent involvement in a potential decompression sickness occurrence.

THE LYMPHATIC SYSTEM AS A PATH TO TRANSFER MICROBUBBLES

One of the functions of the lymphatic system is the maintenance of the fluid balance in the internal environment. Indeed, plasma enters the interstitial spaces from blood flowing into the capillaries. Much of this interstitial fluid is absorbed by tissue cells or reabsorbed by the blood before it flows out of the tissue, but a small amount of interstitial fluid remains inside. Then, lymphatic vessels collect the excess fluid and return it to the venous blood.

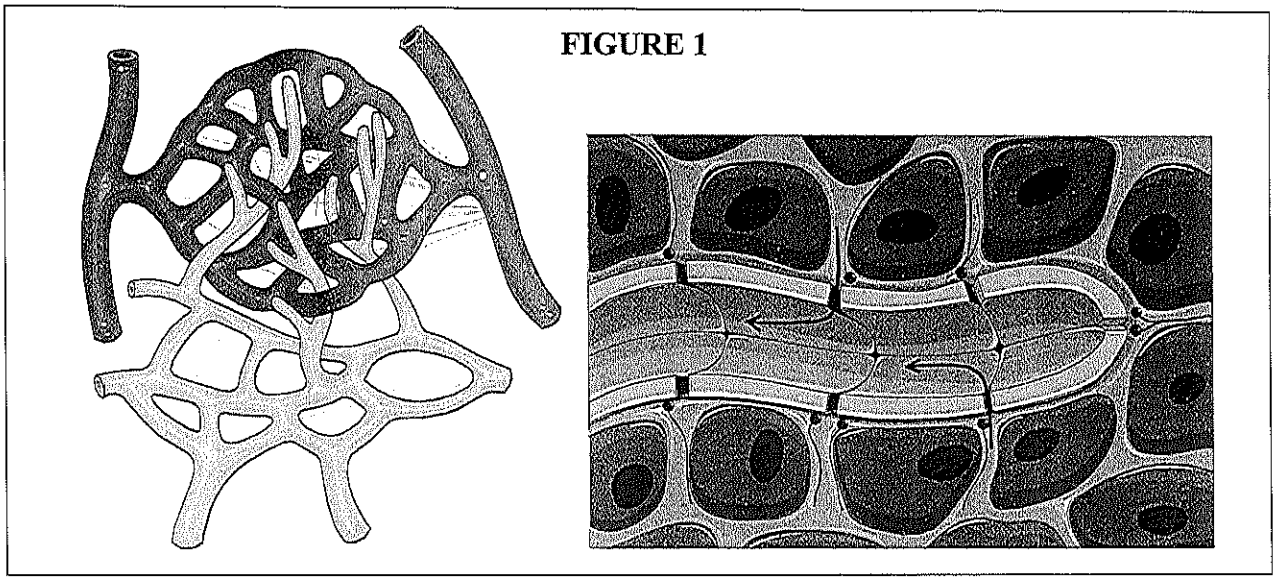

Figure 1. Schematics of the lymphatic capillaries in tissues: conformation with blood capillaries and details.

The lymphatic system is thus a specialized part of the circulatory system that consists of:
1) a moving fluid, the lymph, derived from the blood and tissue fluid; and
2) a group of vessels, the lymphatics, mainly parallel to the veins, that returns lymph to the blood.
Two to three liters/day of interstitial fluid return to the blood circulation.

Let's travel with the lymph inside the lymphatic network from the tissues to the blood (cf. *Figure 2,* Page 228). We propose to discuss here the possibility that microbubbles can be pumped from the tissues' interstitial fluid by the lymphatics and then enter the lymphatic circulation, to be potentially ejected in the venous blood with the lymph return.

The lymphatic system, contrary to the blood circulatory system, does not form a closed loop. It begins blindly in the intercellular spaces of the body tissues (cf. *Figure 1,* above). Networks of lymphatic capillaries are well distributed throughout the body (cf. Figure 2). These capillaries vary in diameter from 15 to 75 microns (47). The high permeability of lymphatic capillaries permits large molecular weight substances that cannot be absorbed by the blood capillaries to be removed from the interstitial spaces. Thus, each day, about 50% of the total blood protein leaks out of the capillaries into the tissue fluid and returns to the blood via the lymphatic vessels.

It is then logical to think that if microbubbles are formed in tissues, the lymphatic system constitutes a favorable path for their transport to the blood. Indeed, we have discussed above the fact that the great majority of the blood capillaries' endothelium is not really permeable; because of this only nanometric entities at best can pass through the gaps between tissues and blood, with an exception for the tissues drained by the sinusoidal capillary network. But the lymphatic capillaries, relatively permeable, should allow the transport of micrometric elements like microbubbles from the tissues to the blood via the lymphatic ducts.

The wall of a lymph capillary is constructed of endothelial cells. At various points along the intercellular junction, the surface membranes are held in close apposition by adhesion devices. But instead of a continuous basement lamina (basement membrane) surrounding this wall, open junctions are frequently observed (48). It has been proposed that these areas between apposing membrane surfaces, which have a lack of attachment devices, represent specialized regions that are easily separated and would permit the passage of excess tissue fluid and large molecules into the lumen of the lymphatic vessel (49). Moreover, there are numerous fine filaments, about 100 A in diameter, that connect the capillaries to the surrounding tissue. These filaments allow a mechanical action on the lymphatic endothelial cells when the tissue intercellular fluid volume and pressure increase.

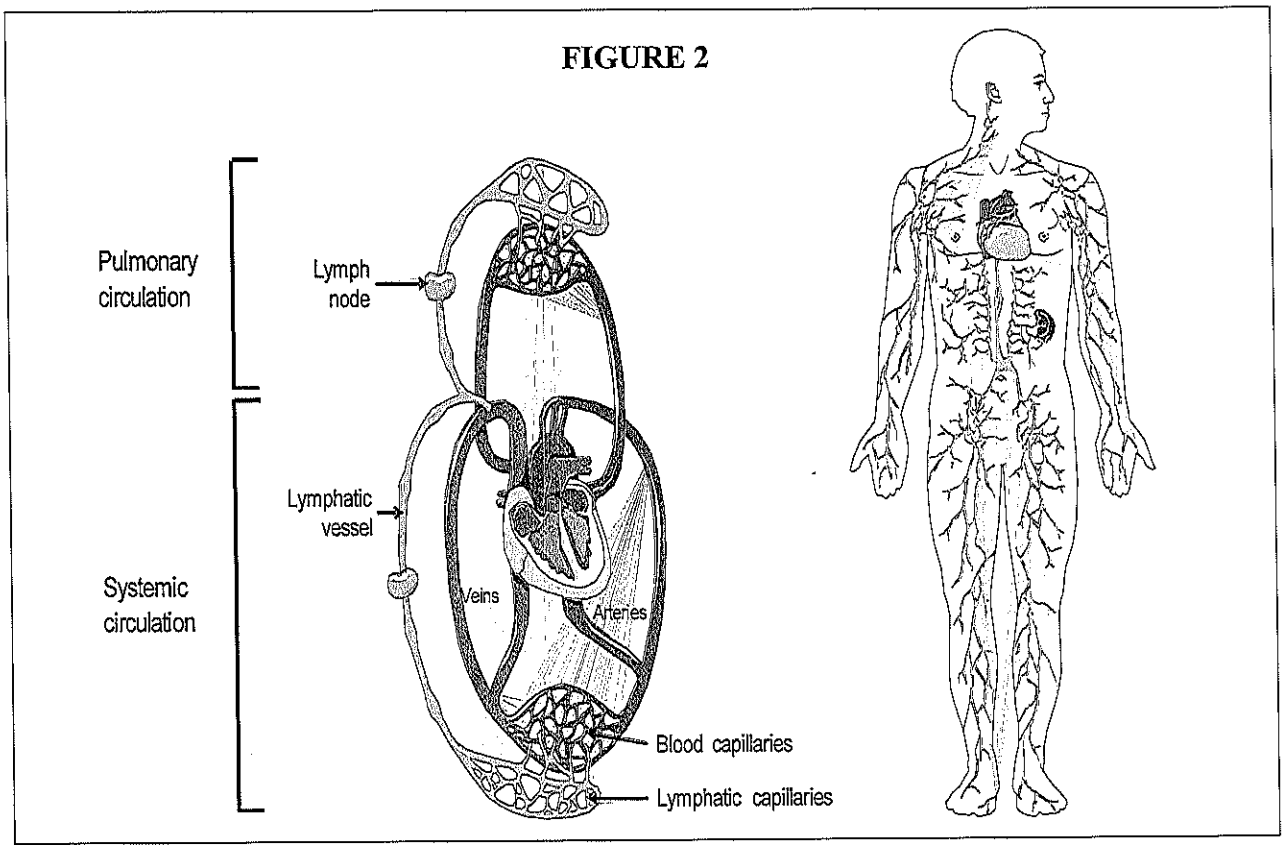

Figure 2. Scheme of the lymphatic/blood networks connections and general view of the lymphatic network

The gaps of the so opened junctions can have dimensions up to several microns. This has been proved in animals (48,50,51). Particles as large as 22.5µm have also been shown capable of passing from the peritoneal cavity into the diaphragmatic lymphatics (52). A more recent work (53) on the mouse describes the fine structure of the specialized junction involving buttons and gaps of micrometric dimensions. To finish, the potential role of vesicles crossing the endothelium and allowing the removal of large molecules has also been discussed (48). So, it is highly probable that microbubbles formed in the interstitial fluid of tissues can pass though the lymphatic endothelium to join the lymph.

It can be remarked that the flow of particles across the lymph capillary endothelium is higher for small particles than for large particles (54). This is an important point because a filtering role of the lymphatics could exist if the gas nuclei population recruited to form microbubbles after a decompression has a wide spectrum of dimensions (35).

Let's continue to follow a potential microbubble pumped from the interstitial fluid and drained by the lymphatic network. Because lymph capillaries have a larger lumen than blood capillaries, the transport of micrometric elements is possible. Downstream, the collecting capillaries and the ducts reach millimetric dimensions. At certain locations, lymphatics enter lymph nodes (cf. *Figure 3*, right). The normal young adult body contains around 450 lymph nodes (47). Lymph nodes have an average diameter of 4mm. Any fluid absorbed by the lymphatic system passes through at least one lymph node before its return to the circulation. As the lymph flows through the lymph sinuses within the tissue of the lymph node, it is filtered. Fixed macrophages remove bacteria, other foreign matter and debris.

The lymphatic tissues of lymph nodes serve also as the sites of the final stages of maturation for some types of lymphocytes and monocytes coming from the bone marrow. These white cells are added to the lymph as it flows through the sinuses of a lymph node. Lymphatics from the lower portion of the

body converge to form a dilated lymph vessel, the cisterna chyli, in the lumbar region of the abdominal cavity. Since phagocytic cells in the sinuses serve as filters for particles and destroy them, it is possible that traveling microbubbles can interact with them. But we could expect this only partially. It is so highly probable that if these structures allow the transfer of lymphocytes, microbubbles can circulate in the whole lymphatic network to be finally ejected into the venous return bloodstream upstream from the heart.

The lymphatic capillaries' arrangements in tissues are varied: They occur singly, in plexuses or arranged in cylinders, as in muscles. They merge with other lymphatics to eventually form the main lymphatic trunks: 1) the right lymphatic duct, which receives lymph from the upper- right quadrant and flows out into the right subclavian vein; and 2) the thoracic duct, where the lymph from the entire body (except for the upper-right quadrant) drains and flows into the venous blood at the junction of the left subclavian and the internal jugular veins. At the termination, a bicuspid valve faces into the vein to prevent or reduce reflux of blood.

The thoracic duct is around 5 mm in diameter at its abdominal root point, becomes narrower at mid-thoracic levels and in 50% of patients grows slightly wider again before its termination (47). Indeed, there is an important structural variability from one person to another. The duct can divide into two vessels which further rejoin, or into branches that form a plexus before joining again to form a short, wide vessel.

Higher in the body, the duct can bifurcate, the left branch ending as usual, the right branch diverging to join one of the right lymph trunks or even the right lymphatic duct, with the combined vessel opening into the right subclavian vein. Kinnaert (55) performed 529 human dissections and described this variability of the thoracic duct termination location (internal jugular, subclavian vein, jugulo-subclavian junction). In 21% of the cases, the terminal openings were multiple. Even if there exists an anatomical variability for these ducts connections among people, the diameter of the duct's termination is so that microbubble passage and final rejection into the bloodstream should be particularly easy (several mm).

FIGURE 3

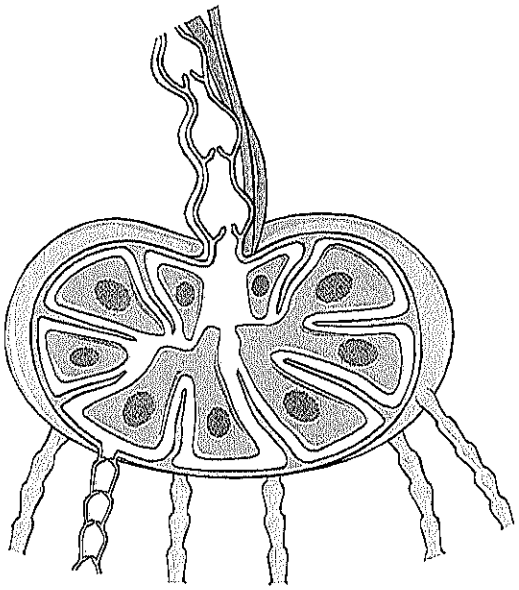

Figure 3. Schematic of a lymph node

Although there is no muscular pumping element connected with the lymphatic vessels to force lymph onwards, this latter moves slowly along its vessels. Lymph flows through the thoracic duct and rejoins the general circulation at the rate of around 100 ml/h. It moves through the system in the right direction because of the large number of valves that allow fluid flow only in one direction. The movement is mainly due to breathing movements, by the motion of adjoining arterioles and by skeletal muscles contractions. This is called the lymphatic pump.

During exercise, lymph flow may increase as much as five to 10 times (56). It is noticeable that movements largely increase the flow of microbubbles that can be detected by a precordial Doppler system after a decompression. This has been attributed to the sudden opening of capillaries with an associated microbubble release in the peripheral network (in skeletal muscles for instance) or to local microcavitations. Nevertheless, the increase of the lymph flow during exercise could also easily explain this phenomenon.

It is interesting to notice that in skeletal muscles, lymphatics are usually paired with arterioles so that vasomotion and arterial pulsations, both with mus-

TABLE 1

Human Lymphatic Vessel or Lymphatic Component	Diameter (mm)	Length (mm)	Wall Thickness	Lymph Flow Rate (mm^3/sec)	Number of Vessels, Tissues or Objects	Total Length (mm)	Total Lymph Volume (mm^3)	Lymph Velocity (μm/s)
Cervical portals:								
Thoracic duct	4.0	450	500μm	21.4	1	450	5700	1700
Right lymphatic duct	3.0	14	500μm	1.7	1	14	100	250
Main lymphatic trunks:								
Subclavian (left and right)	2.5	50	~300 μm	0.7	2	100	550	100
Jugular (left and right)	2.3	40	~300 μm	0.7	2	80	330	200
Intestinal	2.3	85	~300 μm	14	1	85	350	3400
Bronchomediastinal (left and right)	2.2	125	~300 μm	2	2	250	950	500
Lumbar (left and right)	1.9	100	~300 μm	0.3	2	100	570	100
Cisterna chyli (thoracic)	8-13	50-75	~500 μm	14	1	60	1700	500
Minor lymphatic trunks:	1.0	10	~100 μm	0.2	100	1000	800	300
Post-Lymphonodal collecting ducts	0.5	~3	15-50μm	0.01	1700	5100	1000	70
Pre-Lymphonodal collecting ducts	0.5	~3	15-50μm	$4*10^{-5}$	617000	1850000	363000	0.2
Precollecting ducts	0.15	~1	~5 μm	$3*10^{-7}$	68000000	68000000	1200000	0.02
Lymphatic capillaries	0.02	0.5	1μm	$3*10^{-7}$	6800000000	3400000000	425000	0.03
Lymphatics subtotal				23.1		~3500 km	2000000	~10 (avg)
Pre-lymphatic channels	0.1-0.2μm	30μm-30cm		$3*10^{-14}$	$8*10^{14}$	$24*10^{12}$	(370000)	0.002
Lymphocytes	10μm				$8*10^{11}$	-	(350000)	-
Lymph nodes	4			0.05	450	-	(15000)	10
Spleen	66				1	-	(75000)	-
Thymus	22				1	-	(10000)	-
Lymphatic vessel walls					-	-	(460000)	-
Total Lymphatic System							~3300000	

estimated for hypothetical adult male, weight 70kg

Table 1. Approximate quantification of the human lymphatic system (47) © Robert A. Freitas Jr., all rights reserved. Reprinted with permission http://www.nanomedicine.com/NMI.htm

cle contractions, allow the lymph circulation (57). These links with the arterial side could also imply interesting gas exchange patterns between the vessels when pure oxygen is breathed. The impact on the microbubbles circulating in such lymphatics could be non-negligible.

Freitas proposes an approximate quantification of the lymphatic system (47). The corresponding table, inspired from various sources, is reprinted hereafter (cf. *Table 1,* above). According to this data, taking into account the vessel crossing times (~length/velocity), it takes around 24 hours for a node-inert particle entering a lymphatic capillary to reach the termination of the thoracic duct and so rejoin the venous flow. Nevertheless, elsewhere, it has been measured by video microscopy in man that the fluid speed in microlymphatics is close to 10μm/s (7 and 14μm/s for upper and lower quartiles, respectively) at rest (58).

Another recent study proves also that the lymph transit time from hand to axilla in human subjects at rest can be as high as 9cm min-1 (59). Moreover, the flow velocity in the thoracic and in the right lymphatic ducts are non-negligible (10cm/min and 1.5cm/min according to Table 1). Consequently, the microbubbles formed in a proximal zone of the body with regard to the ducts have the opportunity to be drained by the lymphatics and be so transported up to one of the main ducts quite rapidly. It could take no more than a few minutes for microbubbles formed during a decompression in these proximal zones to be ejected into the venous return.

The emerging microbubble flow rate would progressively increase because a greater number of microbubbles recruited from deeper territories could then be involved. This phenomenon would reach a steady state, of greater or lesser duration, depending on the exposure and the decompression procedure chosen, and finally decrease. Indeed, after the decompression, a progressive microbubble reabsorption is generally expected. This is due to the desaturation of the whole body from which tissues associated to the

lymphatic capillary network are a part. This is exactly what is observed with a Doppler: a microbubble peak often around one hour, followed by a progressive fall, when the bubble grade of decompressed divers is evaluated on a long period after surfacing.

Another fundamental consequence of the mechanism proposed here is the following: Microbubbles transferred into the venous bloodstream up to the pulmonary filter will grow during such travel only if the inert gas partial pressure of the mixed venous blood, a contribution of all body organs, is greater than their internal inert gas partial pressure. The lymph content in the thoracic duct being the result of the interstitial fluid of all the drained tissues, a greater proportion of rapid compartments with regard to the venous return now implies that the stabilized microbubbles so transported can emerge in a supersaturated medium for a long period when they reach the blood. A criterion linked to such a growing or crushing condition, time-dependent and involving a whole body gas exchange approach, could give new predictive possibilities for a mathematical model of decompression.

To justify the remark concerning the rapid tissues' contribution in the thoracic duct, it can be said that 30% to 50% of the total lymphatic flow comes from the liver, and 20% to 30% comes from the intestines. While on an empty stomach, the cisterna chyli flow rate is less than 1ml/h, it can increase up to 200ml/h after a fatty meal (60). The corresponding milky intestinal lymph contains a surge of emulsified fat, which is transported in the form of chylomicrons measuring 0.5-0.75 microns in diameter, named chyle (47). In around 35% of cases, the intestinal trunk joins the left lumbar trunk and there is no cisterna chyli. This is another anatomical variability that could be related to the inter-individual variability to accumulate microbubbles in the blood flow after the same exposure. Microbubbles formed in or around the intestines could be transported by the corresponding lymphatic capillary network, linked to chylomicrons whose lipid content is a way to feed microbubbles with inert gas. The literature on the effect of the digestion on microbubble formation after diving is rare.

However, most of the time, lymph has basically the same composition as the interstitial fluid. It contains a lot of proteins and elements (almost no platelets but one-third the fibrinogen and five times the prothrombin as in blood serum) that could interact with a microbubble and stabilize its gas/lymph interface. The biochemical and hematological effects specific to blood-bubble interaction are complex but have been discussed (61). Lymph/bubble interaction effects are rather unknown, probably dependent of the region that is crossed (the biochemical and cellular content of the thoracic duct, of muscular lymph and of hepatic lymph is, for instance, different). To conclude, microbubbles in lymphatics are probably stabilized but the different levels of supersaturation of each converging vessels necessarily imply inert gas exchanges at the lymph/bubble interface; microbubbles volume probably changes during the travel inside the lymphatic network.

To finish, it is an important fact that lymph capillaries branch, interconnect and extend into almost all tissues of the body except the central nervous system and the avascular tissues such as the epidermis and the cartilage. Neither brain nor spinal cord but also parts of articulations are drained so that autochthonously formed microbubbles cannot be transported for further absorption in the venous blood as with other tissues (muscular and adipose tissues, for instance). Symptoms could be also associated to such stationary bubbles and explain partly type I and type II forms of decompression sickness.

CONCLUSION

This paper has presented different mechanisms that have been proposed up to now to explain the fact that microbubbles routinely circulate in large quantities in the venous return. Some of the more interesting have been discussed. How they are formed and how they are transferred into the bloodstream is of primary interest for those who intend to describe the mechanisms of decompression and prevent decompression sickness with efficiency. By highlighting the anatomical and hydrodynamic specificities of the lymphatic system and by assuming that the bulk of the interstitial fluid around the cells represent a large pool volume for microbubble formation, we have proposed that lymphatics drain such microbubbles up to the venous return, via collectors, lymph nodes and ducts. After decompression, the microbubbles so formed in tissues could be progressively transferred to the lymphatics, stabilized and finally ejected into the venous blood. Even if peripheral bubbles have been detected by Doppler (62, 6), supporting the idea that microbubbles can form in the blood

capillary network, it is proposed here that numerous microbubbles are rather formed in tissues and are transported by the slow lymphatic circulation. Then, they can be detected with a Doppler during hours following a decompression, even after moderate hyperbaric exposures (63). This mechanism of microbubble transfer into the bloodstream doesn't exclude the others but could be predominant.

■

ANNEX

We will note hereafter P_{v_mix} the mixed venous blood inert gas partial pressure and P_{amb} the ambient pressure.

As an example, we will choose Levitt's PBPK approach and physiological data to model inert gas exchanges in the body (64). Figure 4 (*right*) illustrates the corresponding tissues arrangement.

We intend to lead a first-order analysis of the cardiac valves involvement using Levitt's tissue flow rates and perfusion limited approach, even if only applied on his study for a standard human at rest, in dry and normoxic conditions. At each instant, we can write, in the course of an air dive, including the decompression:

$$P_{v\_mix} = \frac{\sum_{i=1}^{N} \dot{Q}_i \, Pp_{N_2 i}}{\dot{Q}_{tot}} \qquad (1)$$

where the indice i refers to a specific compartment having a $\dot{Q}_i$ blood flow rate, $\dot{Q}_{tot}$ being the cardiac output and $Pp_{N_2}{}^i$ its inert gas partial pressure.

The authors are aware that the blood flow rates values and distribution at rest/dry conditions and during a dive, with a moderate exercise level, are different (65, 66) but prefer to not consider such complex aspect in this simplified analysis.

FIGURE 4

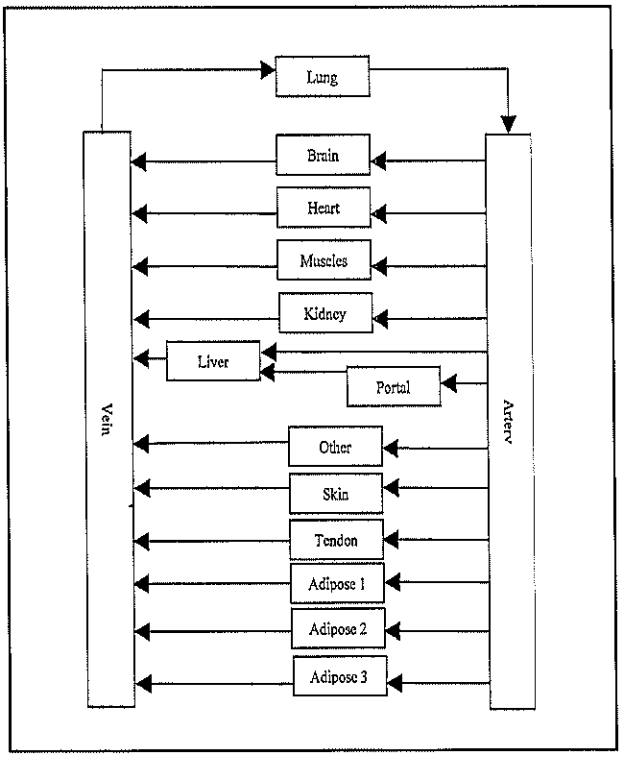

Figure 4. Schematic diagram of the arrangement of the different tissues in Levitt's PBPK model (64). Reprinted with permission

Figure 5 (*facing page, top*) illustrates how the different nitrogen partial pressures and P_{v_mix} varies during a given air exposure (30m/15min). It is clear that the decrease of the mixed venous blood inert gas content during the first minutes of a decompression reflects the fast tissues' behavior. This trend could be moderated because the diver's slight level of activity during the ascent can limit the fast partial pressure decrease of the mixed venous blood (stronger contribution of muscles flow rate to the venous return).

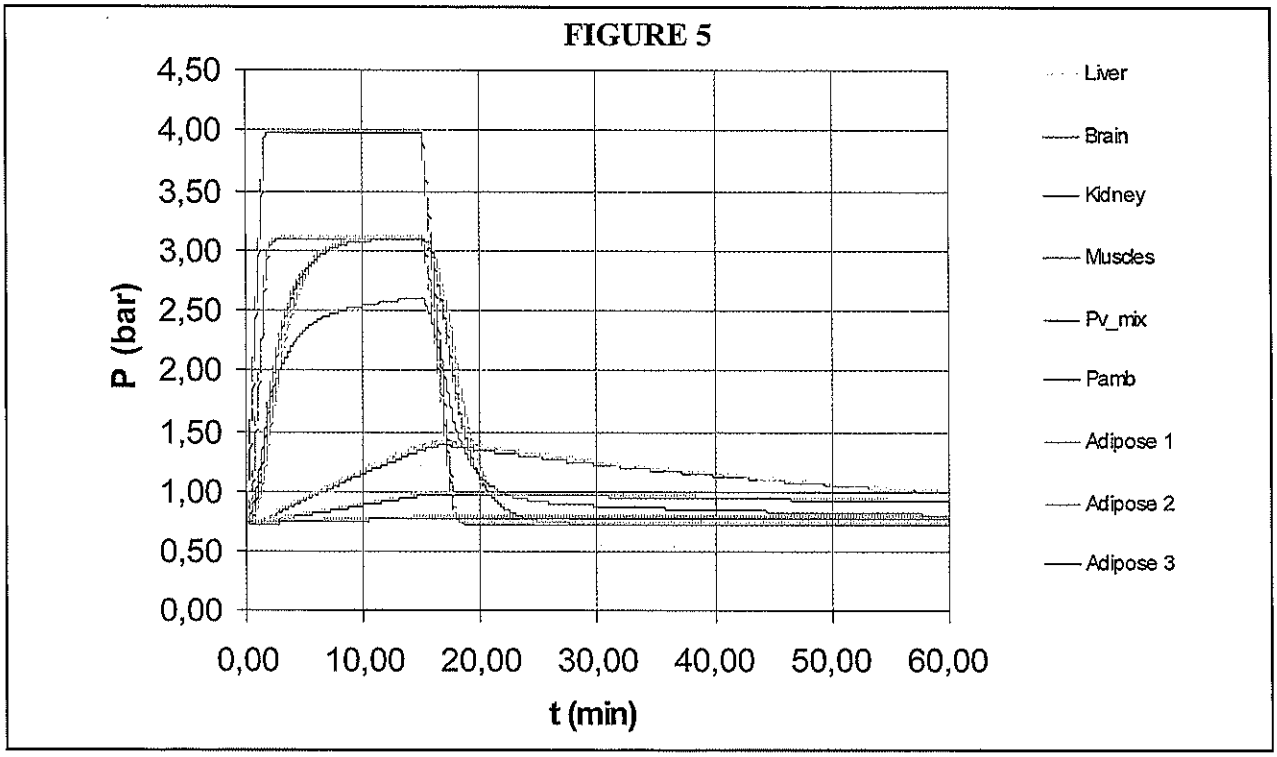

Figure 5. Nitrogen partial pressures and ambient pressure variations for a 30-meter/15-minute air dive (descent rate 20m/min and ascent rate 12m/min), according to Levitt's PBPK approach and using standard values for nitrogen solubilities in oil and water (67)/

It is important to specify what we call a supersaturation state: A gas nuclei is no more stabilized by surface-active molecules and will grow by a diffusion process due to the supersaturated state of the surrounding fluid if its radius r_b is so that:

$$r_b > r_c = \frac{2\gamma}{P_{ss}} \qquad (2)$$

where r_c is defined as the critical radius, g is the surface tension of the surrounding fluid and

$$P_{SS} = P_{v\_mix} - (P_{amb} - \beta) \qquad (3)$$

is the supersaturation pressure. b is the sum of venous metabolic gases (oxygen and carbon dioxide) and the water vapor partial pressures. Following Van Liew (68), for a wide range of arterial oxygen partial pressure going up to 2 atm, the sum of venous oxygen and carbon dioxide partial pressures can be assumed constant (40mmHg and 46mmHg respectively).

It is interesting to point out here that, for the example described above, the mixed venous blood is in a supersaturated state between the 16th and the 22nd minute only.

The number of nuclei recruited at the cardiac valves level is probably all the more numerous because the supersaturation level is high (34). Because of this, it should have a great impact to limit P_{ss} during the ascent.

To continue with the implications of Hennessy's proposition, we can use the well-known Epstein and Plesset approach of bubble growth dynamics (69). The equation and the associated assumptions have been clearly presented by Yount (18) and the expression for the bubble radius rate evolution in our context can be formulated as follows :

$$\frac{dr}{dt} = \frac{RTD_b S_b}{r}\left(1 + \frac{r}{\sqrt{\pi D_b t}}\right)\frac{P_{ss} - \frac{2\gamma}{r}}{P_{amb} + \frac{4\gamma}{3r}} \qquad (4)$$

Where R is the perfect gas universal constant, T the temperature (37°C here), D_b is the gas diffusion coefficient in the blood, S_b is the gas solubility in the blood and r is the bubble radius.

Clearly, the rate of growth of a microbubble born from an activated micronuclei is all the more higher than the supersaturation level of the surrounding medium is high (blood, in this case), but also all the more important becausethat the ambient pressure is low. ❑

References

1. Kisman KE, Masurel G, Lagrue D, Le Pechon JC. Evaluation de la qualité d'une décompression basée sur la détection ultrasonore de bulles. Med Aero Spat, Med Sub Hyp 1978; 67: 293-297.

2. Nishi RY, Kisman KE, Eatock BC, Buckingham IP, Masurel G. Assessment of decompression profiles and divers by Doppler ultrasonic monitoring. In: Bachrach J, Matzen MM, eds. Proc Seventh Symp Underwater Physiol, Undersea Medical Society, Bethesda, Maryland, 1981: 717-727.

3. Nishi RY, Eatock BC. The role of ultrasonic bubble detection in table validation. In: Schreiner HR, Hamilton RW, eds. Validation of Decompression Tables, 37th Undersea and Hyperbaric Medical Society Workshop, Bethesda, Maryland, 1989: 133-137.

4. Nishi RY. Doppler evaluation of decompression tables. In: Lin YC, Shida KK, eds. Man in the Sea, Volume 1, Best Publishing Company, 1990: 297-316.

5. Sawatzkty KD, Nishi RY. Assessment of inter-rater agreement on the grading of intravascular bubble signals. Undersea Biomed Res 1991; 18: 373-396.

6. Spencer MP. Decompression limits for compressed air determined by ultrasonically detected blood bubbles. J Appl Physiol 1976; 40(2): 229-235.

7. Butler BD, Hills BA. The lung as a filter for microbubbles. J Appl Physiol: Respirat Environ Exercise Physiol 1979; 47(3): 537-543.

8. Hennessy TR. On the site of origin, evolution and effects of decompression microbubbles. In: Brubakk AO, Hemminsen BB, Sundnes G, eds. Supersaturation and Bubble Formation in Fluids and Organisms, The Kongsvoll Symposium, 1988 ; Tapir Publishers, 1989: 292-332.

9. Francis TJR, Gorman DF. Pathogenesis of the decompression disorders. In: Bennett P, Elliott D, eds. The Physiology and Medicine of Diving; Fourth Edition; Saunders, 1993: 454-480.

10. Van Liew HD, Burkard ME. Density of decompression bubbles and competition for gas among bubbles, tissue, and blood. J Appl Physiol 1993; 75(5): 2293-2301.

11. Yount DE, Hoffman DC. On the use of a bubble formation model to calculate diving tables. Aviat Space Environ Med 1986; 57 : 149-156.

12. Gernhardt ML. Development and evaluation of a decompression stress index based on tissue bubble dynamics Thesis, University of Pennsylvania, 1991.

13. Van Liew HD, Burkard ME. Bubbles in circulating blood : stabilization and simulations of cyclic changes of size and content. J Appl Physiol 1995; 79(4): 1379-1385.

14. Chappell MA, Payne SJ. A physiological model of the release of gas bubbles from crevices under decompression. Respir Physiol Neurobiol 2006; 153: 166-180.

15. Harvey EN. Decompression sickness and bubble formation in blood and tissues. Bulletin of The New York Academy of Medicine 1945; 21: 505-536.

16. Harvey EN, Barnes DK, McElroy WD, Whiteley AH, Pease DC, Cooper KW. Bubble formation in animals : I. Physical factors. J Cell Comp Physiol 1944; 24(1): 1-22.

17. Tikuisis P. Modelling the observations of in vivo bubble formation with hydrophobic crevices. Undersea Biomed Res 1986; 13(2): 165-180.

18. Yount DE. Growth of gas bubbles from nuclei. In: Brubakk AO, Hemminsen BB, Sundnes G, eds. Supersaturation and Bubble Formation in Fluids and Organisms, The Kongsvoll Symposium, 1988 : Tapir Publishers, 1989: 131-177.

19. Hills BA. A hydrophobic oligolamellar lining to the vascular lumen in some organs. Undersea Biomed Res 1992; 19(2): 107-120.

20. Brubakk AO. Endothelium and bubble injury: the role of endothelium in decompression illness. In: Grandjean B, Meliet JL, eds. 30th Annual Scientific Meeting of the European Underwater Baromedical Society, Ajaccio, Corsica, France, 2004: 17-22.

21. Gratton J-P, Bernatchez P, Sessa WC. Caveolae and caveolins in the cardiovascular system. Circ Res 2004; 94: 1408-1417.

22. Ligier-Belair G, Parmentier M, Jeandet P. Modeling the kinetics of bubble nucleation in Champagne and carbonated beverages. J. Phys. Chem. 2006; 110: 21145-21151.

23. Hayward AJT. Tribonucleation of bubbles. Brit J Appl Physics 1967; 18: 641-644.

24. Ikels KG. Production of gas bubbles in fluids by tribonucleation. J Appl Physiol 1970; 28(4): 524-527.

25. McDonough PM, Hemmingsen EA. Bubble formation in crabs induced by limb motions after decompression. J Appl Physiol 1984; 57(1): 117-122.

26. Lee H, Taenaka Y, Kitamura S. Mechanism for cavitation in the mechanical heart valve with an artificial heart: nuclei and viscosity dependence. Artif Organs 2005; 29:41-46.

27. Milo S, Rambod E, Gutfinger C, Gharib M. Mitral mechanical heart valves : in vitro studies of their closure, vortex and microbubble formation with possible medical implications. Eur J Cardiothorac Surg 2003; 24(3): 364-370.

28. Bachmann C, Kini V, Deutsch S, Fontaine AA, Tarbell JM. Mechanisms of cavitation and the formation of stable bubbles on the Bjork-Shiley Monostrut prosthetic heart valve. J Heart Valve Dis 2002; 11(1):105-113.

29. Herbertson LH., Manning KB, Reddy V, Fontaine AA, Tarbell JM, Deutsch S. The effect of dissolved carbon dioxide on cavitation intensity in mechanical heart valves. J Heart Valve Dis 2005; 14(6):835-842.

30. He Z, XI B, Zhu K, Hwang NH. Mechanisms of mechanical heart valve cavitation : investigation using a tilting disk valve model. J Heart Valve Dis 2001; 10(5): 666-674.

31. Andersen TS, Johansen P, Paulsen PK, Nygaard H, Hasenkam JM. Indication of cavitation in mechanical heart valve patients. J Heart Valve Dis 2003; 12(6):790-796.

32. Johansen P. Mechanical heart valve cavitation. Expert Rev Med Devices 2004; 1(1): 95-104.

33. Franc JP et al. La cavitation – Mécanismes physiques et aspects industriels. Presses Universitaires de Grenoble, 1995.

34. Yount DE, Strauss RH. Bubble formation in gelatin: a model for decompression sickness. J Appl Phy 1976; 47(11): 5081-5089.

35. Yount DE. Skins of varying permeability: a stabilization mechanism for gas cavitation nuclei. J Acoust Soc Am 1979; 65(6): 1429-1439.

36. Yount DE, Yeung CM, Ingle FW. Determination of the radii of gas cavitation nuclei by filtering gelatin. J Acoust Soc Am 1979; 65(6): 1440-1450.

37. Yount DE, Yeung CM. Bubble formation in supersaturated gelatin : a further investigation of gas cavitation nuclei. J Acoust Soc Am 1981; 69(3): 702-708.

38. Hills BA. A thermodynamic and kinetic approach to decompression sickness. Thesis, Adeliaïde, Libraries Board of South Australia, 1966.

39. Yount DE, Hoffman DC. On the use of a bubble formation model to calculate diving tables. Aviat Space Environ Med 1986; 57 : 149-156.

40. Blatteau J-E, Hugon M, Gardette B. Deep stops during decompression from 50 to 100msw didn't reduce bubble formation in man. UHMS Workshop "Decompression and the Deep Stop" 24-25 June 2008.

41. Nikolaev VP. Effects of heterogeneous structure and diffusion permeability of body tissues on decompression gas bubble dynamics. Aviat Space Environ Med 2000; 71: 723-729.

42. Yount DE. Application of a bubble formation model to decompression sickness in rats and humans. Aviat Space Environ Med 1979; 50(1): 44-50.

43. Rippe B, Rosengren B-I, Carlsson O, Venturoli D. Transendothelial transport : the vesicle controversy. J Vasc Res 2002; 39: 375-390.

44. Gil J, Silage DA. Morphometry of pinocytotic vesicles in the capillary endothelium of rabbit lungs using automated equipment. Circ Res 1980; 47: 383-391.

45. Renkin EM. Multiple pathways of capillary permeability. Circ Res 1977; 41: 735-743.

46. Middleton J, Patterson AM, Gardner R, Schmutz C, Ashton BA. Leukocytes extravasion : chemokine transport and presentation by the endothelium. Blood 2002; 100(12): 3853-3860.

47. Freitas RA. Nanomedicine Volume I: Basic Capabilities, Landes Bioscience, Georgetown, TX, 1999.

48. Leak LV. Sudies on the permeability of lymphatic capillaries. J Cell Biol 1971; 50: 300-323.

49. Leak LV, Burke JF. Fine structure of the lymphatic capillary and the adjoining connective tissue area. Am J Anat 1966; 118(3): 785-809.

50. Trzewik J, Mallipattu SK, Artmann GM, Delano FA, Schmid-Schönbein GW. Evidence for a second valve system in lymphatics: endothelial microvalves. FASEB J 2001; 15: 1711-1717.

51. Ikomi F, Hunt J, Hanna G, Schmid-Schönbein GW. Interstitial fluid, plasma protein, colloid, and leukocyte uptake into initial lympatics. J Appl Physiol 1996; 81(5): 2060-2067.

52. Allen L. On the penetrability of the lymphatics of the diaphragm. Anat Record 1956; 124(1): 639-652.

53. Baluk P et al. Functionaly specialized junctions between endothelial cells of lymphatic vessels. J Exp Med 2007; 204(10): 2349-2362.

54. Ikomi F, Hunt J, Hanna G, Schmid-Schönbein GW. Mechanism of colloïdal particle uptake into the lymphatic system : basic study with percutaneous lymphography. Radiology 1995; 196: 107-113.

55. Kinnaert P. Anatomical variations of the cervical portion of the thoracic duct in man. J Anat 1973; 115: 45-52.

56. Havas E et al. Lymph flow dynamics in exercising human skeletal muscle as detected by scintography. J Physiol 1997; 504(1) : 233-239.

57. Schmid-Schönbein GW. Mechanisms causing initial lymphatics to expand and compress to promote lymph flow. Arch Cytol Histol 1990; 53: 107-114.

58. Fischer M et al. Flow velocity of single lymphatic capillaries in human skin. Am J Physiol 1996; 270: H358-63.

59. Modi S et al. Human lymphatic pumping measured in healthy and lymphoedematous arms by lymphatic congestion lymphoscintigraphy. J. Physiol 2007; 583(1): 271-285.

60. Caumartin J, Dujardin T. L'ascyte chyleuse postopératoire en urologie. Progrès en Urologie 2005; 15: 1046-1055.

61. Hallenbeck JM, Bove AA, Elliott DH. The bubble as a non mechanical trigger in decompression sickness. In: Blood-bubble interaction in decompession sickness, DCIEM Conference, Proceedings n°73-CP-960, ed. KN Ackles, 1973: 129-139.

62. Spencer MP, Clarke HF. Precordial monitoring of pulmonary gas embolism and decompression bubbles. Aerospace Med 1972; 43(7): 762-767.

63. Masurel G. Contribution à l'étude du role physio-pathologique des bulles générées chez l'animal et chez l'homme par un séjour en atmosphere hyperbare. Thesis, Université Claude Bernard – Lyon 1, 1987.

64. Levitt DG. Heterogeneity of human adipose blood flow. BMC Clinical Pharmacology 2007; 7:1.

65. Balldin UI, Lundgren CEG, Lundvall J, Mellander S. Changes in the elimination of 133Xenon from the anterior tibial muscle in man induced by immersion in water and by shifts in body position. Aerospace Med 1971; 42: 489-493.

66. Balldin UI. Effect of immersion and ambient temperature on elimination of 133Xenon from human adipose tissue In: Shilling&Beckett eds. Proc. Sixth Symp. Underwater Physiol., Societies of Experimental Biology, 1978: 329-334.

67. Lango T, Morland T, Brubakk AO. Diffusion coefficients and solubility coefficients for gases in biological fluids and tissues: a review. Undersea Hyp Med 1996 ; 23(4): 247-272.

68. Van Liew HD, Conkin J, Burkard ME. The oxygen window and decompression bubbles: estimates and significance. Aviat Space Environ Med 1993; 64: 859-865.

69. Epstein PS, Plesset MS. On the stability of gas bubbles in liquid-gas solutions. J Chem Phys 1950 ; 18(11): 1505-1509.